# Tyrosine Autofluorescence as a Measure of Bovine Insulin Fibrillation

Innocent B. Bekard and Dave E. Dunstan*
Department of Chemical and Biomolecular Engineering, The University of Melbourne, Melbourne, Victoria, Australia

ABSTRACT The traditional approach to investigating the partial unfolding and fibrillation of insulin, and proteins at large, has involved use of the dyes 1-anilinonaphthalene-8-sulphonic acid (ANS) and Thioflavin T (ThT), respectively. We compare the kinetic profiles of ThT, ANS, light scattering, and intrinsic Tyr fluorescence during insulin fibrillation. The data reveal that the sequence of structural changes (dimers → monomers → partially unfolded monomers → oligomeric aggregates → fibrils) accompanying insulin fibrillation can be detected directly using intrinsic Tyr fluorescence. The results indicate that at least two distinguishable structural intermediates precede fibril development. There is no evidence of tyrosinate or dityrosine during insulin aggregation. Obtaining such critical information from the protein itself is complementary to existing aggregation probes and affords the advantage of directly examining structural changes that occur at the molecular level, providing concrete details of the early events preceding fibrillation.

## INTRODUCTION

It is now accepted in the literature that under appropriate solution conditions, proteins have an inherent property of misfolding and forming fibrillar aggregates (1,2). The fibrils so formed are thermodynamically stable and rich in $\beta$-sheets. Understanding protein aggregation is of critical importance to a wide variety of biomedical situations ranging from conformational disorders (such as Alzheimer's disease and cataracts) (3) to the production, stability, and delivery of protein-based pharmaceuticals including insulin and immunoglobulin G (4). Surprisingly, the molecular mechanism underlying protein aggregation is still not fully understood.

Insulin is a 51-residue peptide-hormone involved in the homeostasis of blood glucose levels. It is composed of two peptide chains, A and B, of 21 and 30 amino acid residues, respectively (5). The A-chain contains an intrachain cystine bridge between residues $A^6$ and $A^{11}$ and is covalently linked to the B-chain via two interchain cystine bridges, $A^7$–$B^7$ and $A^{20}$–$B^{19}$ (6). The peptide-hormone derives its stability from these strongly hydrophobic cystine groups (7). The secondary structure of native insulin is reported to be 58% $\alpha$-helical with a 6% $\beta$-sheet region (8). The helical segments span residues $A^1$–$A^9$ and $A^{12}$–$A^{19}$ of the A chain, and $B^9$–$B^{19}$ of the B chain (9–11). Other studies suggest an additional, phenol-promoted helix spanning residues $B^1$–$B^8$ (12). In solution, insulin has the unique trait of assuming different association states, including dimers, tetramers, and hexamers (13). The various association states are dependent on the overall net charge on the protein and hence are dictated by the solution pH. Insulin is hexameric at physiological pH, dimeric in mineral acids, including HCl, and monomeric in 20% acetic acid (6,13). Insulin is conformationally flexible (between the R- and T-states) at physiological pH, but stable under acidic conditions (14).

Since its discovery in 1921, insulin has been isolated and produced in commercial quantities to treat insulin-dependent diabetics (15). A major problem confronting the industry is insulin aggregation during processing and delivery of the protein-drug. Conventional processing of insulin involves exposure of the peptide-hormone to agitation, low pH, and varying shear rates (during filtration, pumping, and centrifugation), as well as to an array of interfaces during administration (4,16). These conditions are known to facilitate conformational destabilization, leading to partial unfolding and subsequent coalescence of insulin into amorphous and/or fibrillar aggregates (17). Indeed, amyloid plaques have been observed in insulin-dependent diabetics after repeated administration of insulin (18) and in normal aging (19).

The abnormal folding and association of a protein into fibrous aggregates is not unique to insulin. This phenomenon has been reported for a range of polypeptides and has received considerable attention in research (20,21). It is proposed that insulin aggregation proceeds through the dissociation of oligomeric states into monomers, which then undergo conformational changes and reassociate into stable, fibrous amyloid aggregates rich in $\beta$-sheets (22). It is thought that the coalescence of partially folded monomers and the emergence of fibrillar insulin is driven primarily by hydrophobic interactions (6,17). An in-depth knowledge of the key steps and contributors to protein aggregation is crucial for the development of therapeutic drugs to circumvent conformational disorders, and will also inform the design of quality control systems in industry to ensure the stability of the physical and chemical integrity of protein products during processing, transportation, and storage.

The traditional approach to investigating the partial unfolding and fibrillation of insulin, and of proteins at large, has involved use of the dyes 1-anilinonaphthalene-8-sulphonic acid (ANS) and Thioflavin T (ThT), respectively.

*Submitted April 2, 2009, and accepted for publication July 23, 2009.*

*Correspondence: davided@unimelb.edu.au

Editor: Kathleen B. Hall.



0006-3495/09/11/2521/11 $2.00

doi: 10.1016/j.bpj.2009.07.064

On interacting with hydrophobic groups, ANS shows a new emission $\lambda_{max}$ at 460 nm upon excitation at 350 nm and has been successfully applied to show that a partially folded intermediate state precedes fibril formation (23). Thioflavin T, on the other hand, is known to associate rapidly with multimeric $\beta$-sheet-containing amyloid fibrils, showing enhanced emission at 482 nm upon excitation at 450 nm (24,25). Although these dyes have proven instrumental in our understanding of protein aggregation, their mode of action and possible contribution to the aggregation process has yet to be fully understood. For this reason, it is essential to apply an array of complementary techniques when studying the complexities of the structural changes that accompany protein aggregation.

Intrinsic protein fluorescence is a sensitive technique that has been exploited in studying the structural, physicochemical, and functional properties of proteins (26). Proteins derive their intrinsic fluorescence from the chromophores phenylalanine, tyrosine, and tryptophan (27). Bovine insulin contains four Tyr and three Phe residues. In the absence of Trp, Tyr dominates the absorption spectrum of proteins to the exclusion of Phe and nonaromatic absorption attributable to cystine, histidine, or the peptide bond (28). It has been found that protein denaturation results in marked uniformity in its fluorescence characteristics (29), and that is what we expected for insulin under the experimental conditions used in this study. We observe a sigmoid in Tyr fluorescence during insulin aggregation; hence, the focus of this work was to investigate the physical and chemical transformations associated with insulin aggregation by means of its intrinsic fluorescence. Multiple probes were employed to better understand the molecular dynamics involved in the process as indicated by intrinsic Tyr fluorescence.

## MATERIALS AND METHODS

### Materials

Bovine insulin and ThT were obtained from Sigma (St. Louis, MO). The hydrophobic probe ANS was purchased from Aldrich (Milwaukee, WI). All other reagents used were of analytical grade.

### Sample preparation

Insulin solutions were prepared by dissolving the peptide directly in 0.1% (v/v) HCl (pH 1.9) to give a concentration of ~0.2 mg/mL. The final insulin concentration was calculated from ultraviolet (UV) absorption at 280 nm, applying a molar extinction coefficient of 5.53 $mM^{-1}$ $cm^{-1}$. For insulin/dye samples, 1-mM stocks of ThT and ANS were prepared by dissolving each dye in double-distilled water and then filtering through a 0.22-$\mu$m filter paper. The final dye concentration in insulin samples was 50 $\mu$M.

### Fluorescence spectroscopy

Fluorescence studies were conducted using a Cary Eclipse fluorescence spectrophotometer (Varian, Palo Alto, CA) equipped with a Peltier unit for stirring and temperature control. All measurements were obtained using a 1-cm quartz cuvette equipped with a 5-mm magnetic stirrer bar (spin rate, ~120 rpm). Multiple wavelengths were used simultaneously to study both intrinsic (Tyr) and extrinsic (ThT/ANS) fluorescent probes during insulin aggregation. For insulin fibrillation, 3 mL of a reaction sample was incubated at 60°C over a period of 22 h. Intrinsic insulin fluorescence was monitored via Tyr molecules using an excitation wavelength of 276 nm, with emission measured at 303/305 nm (kinetic studies), or 280–500 nm (interval scans). Tyrosinate and dityrosine fluorescence were measured using excitation/emission wavelengths of 295/345 nm and 315/410 nm, respectively. ThT fluorescence emission was measured at 482 nm on excitation at 450 nm, whereas ANS fluorescence was probed using excitation and emission wavelengths of 350 nm and 460 nm, respectively.

### Light scattering

Real-time light scattering was measured during bovine insulin aggregation using the fluorimeter described above. The excitation wavelength was set at 600 nm, away from the absorption regions of the chromophores present, and scattered light was measured at 605 nm (shoulder of excitation peak). The data were collected at 5-min intervals using excitation and emission slit widths of 10 nm unless stated otherwise.

### Data analysis

Fluorescence and CD data were further analyzed using phase diagrams as described elsewhere (30,31).

### Atomic force microscopy

Imaging of insulin fibrils was done using an Asylum MFP 3D atomic force microscope (AFM) (Santa Barbara, CA). Aliquots (20 $\mu$L) from insulin samples incubated at 60°C, with stirring for 22 h, were applied to a freshly cleaved mica surface. A time frame of 30 min was allowed for the protein to fix onto the mica. Excess protein solution on mica was rinsed off thoroughly under running MilliQ water and air-dried in a laminar flow cabinet. Imaging was done in air, under ambient conditions, using silicon nitride probes in intermittent contact mode.

### Secondary structure of insulin fibrils

Far-UV circular dichroism (CD) spectra of fibrillated insulin samples were recorded at room temperature using a Jasco J-815 CD spectrometer (Tokyo, Japan). A 100-$\mu$L aliquot of insulin preparations incubated at 60°C, with stirring for 22 h, was scanned in a 0.2-cm quartz cell from 195 to 240 nm. Solvent spectrum was used as the baseline for data collection. The final spectrum of all samples was an average of three independent scans.

### Thermal denaturation/renaturation experiments

The effect of temperature on insulin structure was studied by fluorescence and CD spectroscopy; conducted over a temperature range of 10–95°C using a temperature gradient of 5°C. The concentration of insulin used was ~0.2 mg/mL in all experiments. For intrinsic fluorescence studies, emission scans of Tyr molecules were recorded from 280 to 500 nm in a 1-cm quartz cell using an excitation wavelength of 276 nm. CD spectra for both near- and far-UV were recorded using a Jasco J-815 CD spectrometer. Insulin samples (200 $\mu$L) were scanned in a 0.2-cm cell from 195 to 340 nm using a data interval of 0.1 nm, a bandwidth of 1.0 nm, a response time of 4 s, and a scanning speed of 50 nm/min. Both fluorescence and CD data were collected after a delay time of 5 min at each temperature.

## RESULTS

The kinetics of insulin denaturation, aggregation, and subsequent fibrillation as detected by multiple parameters were normalized to unity (Fig. 1). The amyloid probe ThT and

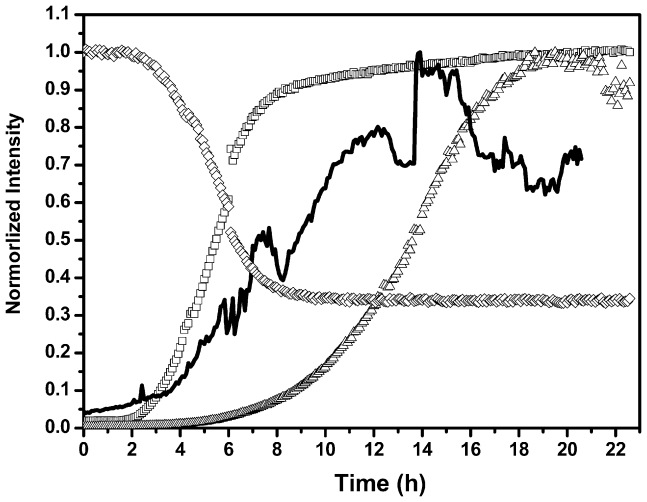


FIGURE 1 Kinetics of insulin fibrillation detected by multiple parameters. Insulin denaturation and subsequent fibrillation were detected by changes in the fluorescence emission of ThT (*open triangles*), Tyr (*open diamonds*), ANS (*open squares*), and light scattering (*solid line*). The experiments were done in 0.1% HCl (pH 1.9) at 60°C, with continuous stirring at 120 rpm.

ANS were employed to detect fibril development and solvent-exposed hydrophobic groups, respectively, during insulin aggregation. Light scattering was used to detect the increase in particle size (aggregates) in solution, and intrinsic Tyr fluorescence provided a means to study the physicochemical changes associated with insulin fibrillation. Reaction samples were incubated at 60°C and stirred continuously at ~120 rpm for 22 h, after which ThT assays, AFM images, and CD spectra confirmed the presence of amyloid fibrils.

## Kinetics of insulin aggregation/fibrillation

The kinetic profile of ThT shows typical sigmoidal behavior indicative of a nucleation-dependent fibril assembly proceeding in three phases (8): 1), a lag phase, during which a fibril-competent nucleus evolves; 2), a growth phase, with rapid polymerization of amyloidogenic nuclei into fibrils; and 3), an equilibrium phase, in which the fibrils mature. The validity of this mechanism of insulin fibrillation is supported by data obtained from complementary studies described below.

A dramatic increase in ANS fluorescence and quenching of Tyr fluorescence was observed to occur in sync at ~2 h of incubation, both reaching equilibrium after 8 h. The two profiles were obtained simultaneously from an insulin-ANS sample. The fluorescence enhancement of ANS at 460 nm indicates the presence of solvent-exposed hydrophobic regions, originating from partially folded intermediates in solution. The concurrent decrease in Tyr fluorescence suggests that Tyr residues were within hydrophobic pockets in the protein matrix and became accessible to effective quenchers upon exposure to the aqueous environment. Indeed, Tyr-$A^{14}$, Tyr-$B^{16}$, and Tyr-$B^{26}$ are resident in the two hydrophobic faces of the insulin monomer that associate to form dimers (32); and the emission intensity at 305 nm is an average of the parametric changes affecting the microenvironment of all Tyr residues. It is worth noting that the lag times for these changes terminated ~3 h before the onset of ThT fluorescence enhancement at 482 nm, which shows that partially folded intermediates indeed precede insulin fibrillation.

The light-scattering profile shows the gradual development of large aggregates (oligomers) in solution from the onset of incubation, with a dramatic increase occurring after ~3 h. This clearly shows that the early insulin aggregates formed, although light-scattering, escape detection by ThT. The data also reveal that the partially folded intermediates, which begin to evolve after ~2 h incubation, associate rapidly into these oligomers from which fibrillar aggregates develop. The occasional spikes experienced in the kinetic trace are attributable to the polydispersed nature of insulin aggregates formed during fibrillation (33,34).

The observed intrinsic Tyr fluorescence profile during insulin fibrillation, relative to those of ThT and ANS, informed the design of an experimental approach to study insulin fibrillation via its intrinsic fluorescence.

## Insulin fibril morphology and secondary structure

AFM height traces of insulin fibrils formed in the presence or absence of dyes is shown in Fig. 2, *a–c*. A dense network of fibrils is observed in all cases, consistent with that reported elsewhere (6). The crowded nature of the fibril network made it difficult to measure heights of individual fibrils relative to the mica surface. However, it is clear by visualizing that fibrils formed in the absence of a dye were thinner than those formed in the presence of ThT or ANS. This observation suggests variations in fibril morphology. The images were made in the order in which they are presented, hence dispelling the possible introduction of an artifact, for example, tip broadening of measured lateral dimensions. Complementary studies using electron microscopy gave similar results (data not shown).

The far-UV spectra of insulin samples incubated for 22 h at 60°C in the presence and absence of ThT/ANS are shown in Fig. 2 *b*. All three spectra were characteristic of $\beta$-sheet secondary structure, but with noticeable differences in trace and minimum ellipticity, depending on the dye present. The spectra obtained for dye-free insulin and insulin-ThT both showed minimum ellipticity at 220 nm, whereas that obtained for insulin-ANS had its peak negative intensity at 222 nm. These minima show a red shift from the characteristic $\beta$-sheet signature, which occurs between 215 nm and 218 nm. The occurrence of this feature can be ascribed to residual helical structure in fibrillar insulin, possibly originating from the B-chain helix (30). It is also possible that the observed differences are a consequence of insulin-dye

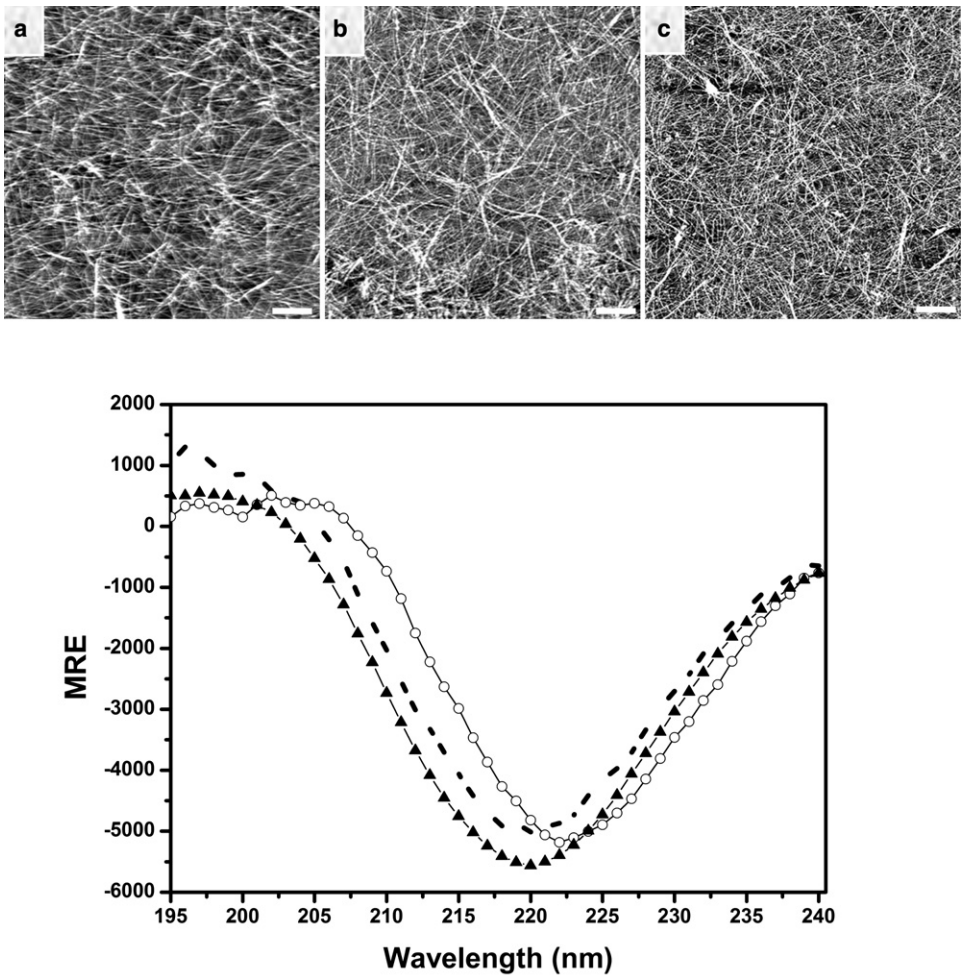


FIGURE 2 Morphology and secondary structure of fibrillated insulin. (*a–c*) AFM height trace images comparing insulin fibrils formed in the presence of ThT (*a*) and ANS (*b*) and in the absence of a dye (*c*). The images show variations in fibril morphology depending on the dye present. Scale bars, 1 $\mu$m. (*Lower*) Far-UV spectra of insulin fibrils at pH 1.9. The spectra represent fibrils formed in the presence of ThT (▲▲▲) and ANS (○), and in the absence of a dye (*dash-dotted line*). The data were collected at ambient temperature, and each trace is an average of three independent scans.

interactions leading to polymorphisms in the resulting fibril structure.

## Monitoring insulin fibrillation via Tyr fluorescence

At ambient temperature, intrinsic Tyr fluorescence of insulin preparations (see Materials and Methods) showed an emission $\lambda_{max}$ at 305 nm with two excitation peaks at 276 nm and 227 nm. This indicates that the freshly prepared reaction solutions did not contain hydrogen-bonded Tyr residues.

Two approaches were used to monitor changes in Tyr fluorescence for a dye-free insulin sample incubated under conditions favoring fibrillation. The aim was to explain the Tyr fluorescence quenching observed during insulin aggregation by probing the possible chemical modifications the fluorophore may access. The first method was to conduct interval scans of the emission spectrum during insulin aggregation (Fig. 3 *a*). The insulin sample was excited at 276 nm, with emission scans from 280–500 nm at 5-min intervals (1-h interval scans are shown for clarity). The scans show a decrease in Tyr fluorescence intensity during insulin fibrillation. This becomes apparent on plotting the emission intensity at 305 nm against time (Fig. 3 *a*, *inset*), which gives a sigmoid curve similar to that of the Tyr fluorescence profile in Fig. 1. The data were further analyzed using phase diagrams, which have proven versatile in detecting intermediate states of a protein undergoing structural transition from an initial to a final state (35). A plot of the emission intensity $I_{330nm}$ against $I_{305nm}$ from the fluorescence data (Fig. 3 *b*) shows three linear segments spanning 0–3 h, 3–12 h, and 12–22 h. Each segment describes a distinctive structural transition, revealing the existence of four structurally unique species during insulin fibrillation. Using information gathered from Fig. 1, we identify the structural species involved as 1), the initial mix of monomers and dimers; 2), partially unfolded intermediates/oligomers; 3), protofibrillar aggregates; and 4), mature fibrils. This observation is consistent with the proposal that structural transitions accompany insulin fibrillation (22,23,36).

The second approach involved monitoring Tyr fluorescence at fixed wavelengths (see the Supporting Material). This allowed simultaneous studies of changes in Tyr fluorescence (excitation 276 nm, emission 305 nm) and the possible formation of tyrosinate (excitation 295 nm, emission

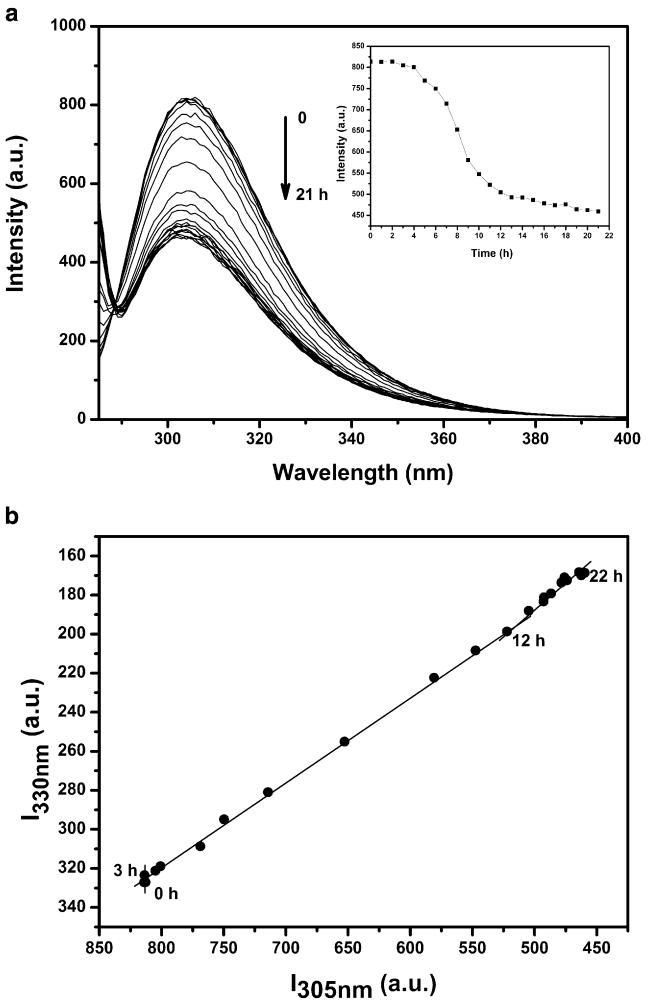


FIGURE 3 Insulin denaturation/fibrillation detected by Tyr fluorescence. (*a*) Fluorescence emission spectra of tyrosine during insulin aggregation. The insulin sample (0.2 mg/mL) was excited at 276 nm, with emission scans from 280 to 500 nm. The figure shows a consistent decrease in intensity of the emission $\lambda_{max}$ (305 nm) after ~2 h of incubation, reaching equilibrium after 12 h. (*Inset*) A sigmoid is observed on plotting the emission intensity at 305 nm against time. (*b*) Fluorescence phase diagram obtained by plotting $I_{330nm}$ against $I_{305nm}$ shows the multiple structural transitions accompanying insulin aggregation. The experiment was done in 0.1% HCl (pH 1.9) at 60°C, with continuous stirring at 120 rpm.

345 nm) and/or dityrosine (excitation 315 nm, emission 410 nm) during insulin aggregation. The intrinsic Tyr fluorescence kinetic profile showed the familiar sigmoid curve (Fig. S1 *a* in the Supporting Material). There was no significant change in the emission intensity at the wavelengths associated with tyrosinate and dityrosine over the 22-h period (Fig. S1, *b* and *c*). The phenol group of Tyr has a pKa of 9.8 and 4.2 for the ground and excited states, respectively (37). At pH 1.9, the phenol group of Tyr and its possible proton acceptors, including Glu and Asp residues, are fully protonated, which explains the absence of tyrosinate, and hence dityrosine, during insulin aggregation. It is noteworthy that the position and shape of the emission spectrum of Tyr in fibrillated insulin solutions showed the same peaks observed in a freshly prepared sample, though considerably diminished in intensity. This reaffirmed that Tyr residues present in the insulin fibrils were nonhydrogen-bonded. Indeed, early studies by Waugh showed that the conversion of native insulin molecules into fibrillar aggregates did not involve chemical modification (38). Recent studies using $\alpha$-synuclein at pH 7.4 found that whereas there was no evidence of dityrosine formation during fibrillation, this covalent linkage was observed in the soluble aggregates present after fibrillation was complete (39).

## Temperature effect on bovine insulin

Thermal denaturation and renaturation of bovine insulin and associated changes in its structure were studied by fluorescence and CD spectroscopy; conducted independently but under comparable experimental conditions. The aim was to further understand the sensitivity and, hence, applicability of intrinsic Tyr fluorescence in studying conformational and structural changes in bovine insulin during aggregation. CD spectra in the far-ultraviolet wavelength range (typically from ~190 to 250 nm) provide useful information on the secondary structure of proteins (40), whereas intrinsic protein fluorescence (in this case Tyr fluorescence) provides basic information on the dynamics of structural reorganization in protein molecules (35). At ambient temperature, the far-UV spectrum of native insulin showed two negative peak intensities at 209 nm and 222 nm, typical of an $\alpha$-helical secondary structure, and these intensities have been used in studying insulin denaturation (41).

Thermal unfolding of the helical segments of insulin was monitored using the ellipticity at 222 nm, whereas Tyr fluorescence emission was monitored from 280 to 500 nm on excitation at 276 nm (the intensity at $\lambda_{max}$ 303 nm is shown) (Fig. 4 *a*). The far-UV spectrum shows that temperature elevation results in a significant decrease in the negative intensity at 222 nm, indicating a loss of helical structure. Such conformational changes obviously would affect the local environment, especially of the three Tyr residues resident in the helical regions of bovine insulin (6). True to this, the Tyr emission intensity at 303 nm showed a 73% decrease as a function of temperature on heating from 10°C to 95°C. It has been established that the emission $\lambda_{max}$ of Tyr is independent of temperature (31) and the location of nonhydrogen-bonded Tyr in a protein's hydrophobic interior or $\alpha$-helical segment enhances its quantum yield (or intensity) (42). Therefore, the observed decrease in Tyr fluorescence intensity is attributable to effective Tyr-quencher interactions facilitated by 1), heat-induced structural disorder of the native state via perturbation of intra-/intermolecular interactions (including hydrogen bonding, van der Waals, hydrophobic, and electrostatic interactions); and 2), enhanced dynamic mobility of the entire protein matrix, dictated by solvent viscosity (29).

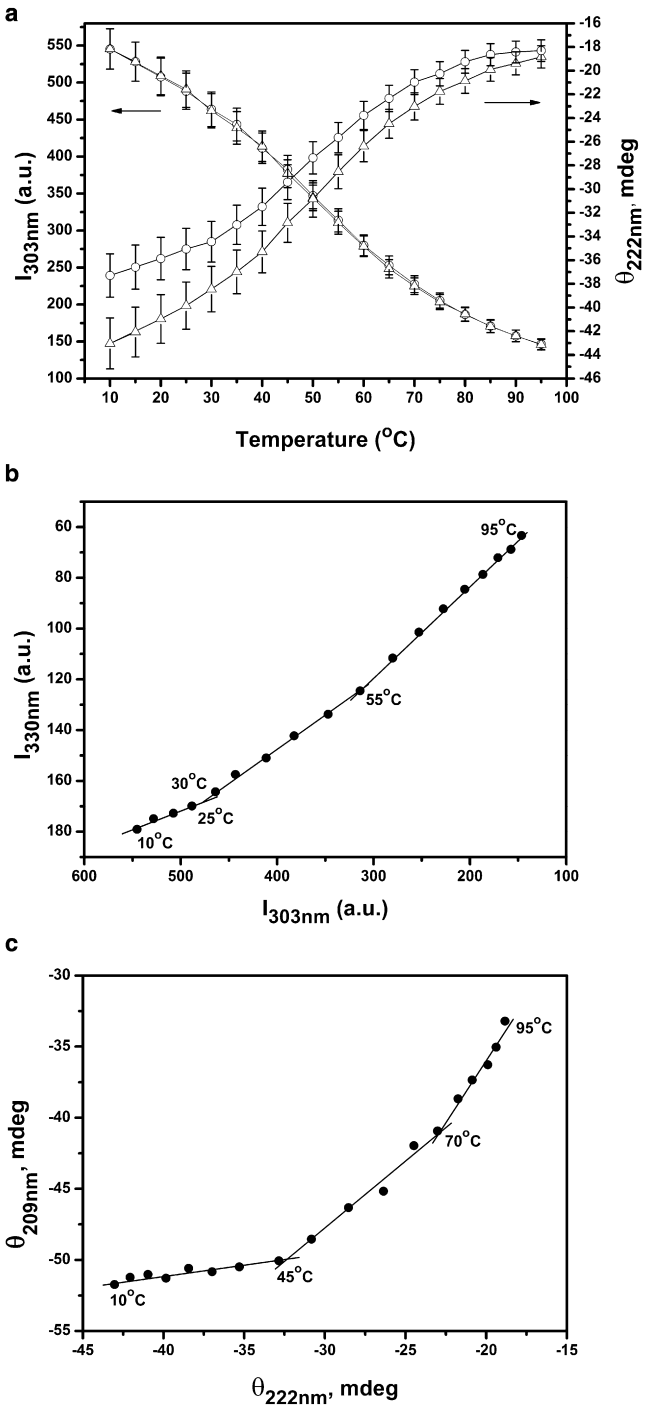


FIGURE 4 Thermal denaturation of bovine insulin (0.2 mg/mL) as detected by fluorescence and CD spectroscopy. (*a*) Decrease in Tyr emission intensity at 303 nm and loss of secondary structure on heat denaturation (*open triangles*). The reverse is observed on renaturation (*open circles*). The temperature range was between 10°C and 95°C, and data were collected at 5°C intervals. Phase diagrams obtained from fluorescence (*b*) and CD (*c*) data reveal the existence of structural intermediates on thermal denaturation of insulin. Error bars indicate the ±SD of duplicates of each experiment.

Both fluorescence and CD spectra show that the major transition occurred between 25°C and 80°C. It is important to note that the fluorescence spectra also show that the transitions involved are completely reversible, as the emission intensities at various temperatures were restored on renaturation. However, the CD spectra on renaturation show ~13% loss in the native helical content (with reference to the intensities at 10°C) which suggests that some molecular interactions were permanently damaged on denaturation, hence preventing the complete refolding of insulin on cooling.

The fluorescence and CD data were further analyzed using phase plots (Fig. 4, *b* and *c*, respectively). Fluorescence phase plots were obtained by plotting $I_{330nm}$ against $I_{303nm}$, whereas CD phase plots were generated using the negative ellipticities at $\theta_{209nm}$ and $\theta_{222nm}$. We chose the peak wavelengths from the CD spectra, as these have been successfully used in building phase plots to distinguish structural transitions during insulin fibrillation (30). Both plots show three linear segments, indicative of the existence of two intermediate states during the transition from native to temporarily denatured insulin. A closer analysis of the plots shows that whereas the linear segments of the fluorescence data span 10–25°C, 30–55°C, and 55–95°C, those of the CD data span 10–45°C, 45–70°C, and 70–95°C. The difference in the temperature range of the linear segments for the two probes indicates that they differ in their sensitivity to structural changes in native insulin, and hence can be applied as complementary techniques in studying insulin denaturation.

The initial transition (10–25°C) in the fluorescence plot may be attributed to a decrease in viscosity of the protein matrix enhancing intramolecular collisions between excited Tyr side chains and neighboring quenchers. The CD plot shows no major conformational change within this temperature range. The second fluorescence transition (30–55°C) corresponds to the dissociation of dimers into monomers and the emergence of the so-called heat-induced molten insulin globule, which is the major species in solution at ~55°C (43). It is noteworthy that this is the first major conformational transition detected by CD (at ~45°C), reaching a maximum at ~70°C. Indeed, differential scanning calorimetry scans of bovine insulin (pH 1.9) showed an endothermic transition midpoint at 60°C (44). Therefore, transitions beyond 55°C can be ascribed to thermal unfolding of monomeric insulin into an unstructured, aggregation-prone intermediate.

It is worth noting that the tertiary/quaternary structure of bovine insulin monitored at $\theta_{278nm}$ (typical Tyr signature) showed complex structural transitions occurring at temperatures similar to that observed in the fluorescence phase plots (data not shown). However, the data were not considered in detail, because the peak negative intensity at 278 nm was weak (near zero), indicating a lack of native tertiary interactions. We attribute this weakness to the low insulin concentration used in this study. This is consistent with the notion that insulin adopts a less rigid structure at low

concentrations, with highly mobile aromatic side chains that show weak intensity. Disulfide bonds, three of which are present in insulin, are known to contribute significantly to the absorption in the near-UV region, which further complicates the interpretation of spectral data obtained from that region (45,46).

## DISCUSSION

The use of fluorescent probes has found wide application in studies of the structure and dynamics of proteins (31). In vitro studies of protein aggregation have employed the histological dye Thioflavin T to detect amyloid fibrils and the hydrophobic dye ANS to establish the existence of partially folded intermediates on the pathway to protein fibrillation (47,48). It is interesting to note that structural changes in proteins can be detected via intrinsic protein fluorescence (31); hence, this feature can be applied (in addition to other techniques) in resolving the complex structural transitions involved in protein aggregation. The main advantage of using intrinsic protein fluorescence is that it provides information on the dynamics associated with protein aggregation at the molecular level. To probe the kinetics of insulin fibrillation via intrinsic fluorescence, it is important to appreciate the underlying cause of the observed Tyr fluorescence quenching and how this feature is related to the fibrillating protein.

### Quenching of Tyr fluorescence during insulin aggregation

There are several possible catalysts for the observed Tyr fluorescence quenching preceding insulin fibrillation: 1), protolysis of the phenol group of Tyr when it interacts with solvent molecules and/or amino acid side chains, which can act as proton donors or acceptors or as hydrogen-bonding partners; 2), resonance energy transfer from Tyr to Tyr, Tyr to tyrosinate, Tyr to ANS, or Tyr to ThT; 3), interactions between the excited chromophore and hydrated peptide carbonyl groups; or 4), interactions between the excited chromophore and cystine groups (49). The occurrence of any of these mechanisms is dependent on the local environment of both the ground and singlet excited states of Tyr residues in the protein matrix, including their proximity to and interactions with quenchers.

The ionizable groups in bovine insulin are fully protonated at pH 1.9. Since excited Tyr residues have a nominal pKa of 4.2, deprotonation of the hydroxy group and subsequent formation of tyrosinate or Tyr-carboxylate hydrogen bonds is theoretically impractical. Our results show that the emission $\lambda_{max}$ of Tyr is constant at 305 nm, although considerably diminished in intensity, even after insulin fibrillation. Further supporting this finding, the kinetic experiments discounted the likelihood of transient hydrogen bonds existing between Tyr residues and solvent molecules, the peptide carbonyl, or neighboring carboxyl groups. This was expected as the rate of depopulation of the excited state by emission is much faster than depopulation by excited-state protolysis (37). Taken together, the observed Tyr fluorescence quenching during insulin aggregation is unlikely to be due to protolysis of the phenolic chromophore in the ground or excited states.

The presence of multiple Tyr and Phe residues in bovine insulin raises the possibility of resonance energy transfer from Phe to Tyr and between adjacent Tyr residues. However, the 276-nm excitation wavelength used in this study would minimize the amount of light absorbed by Phe residues, because these residues show maximum absorption at 258 nm. The radii of globular proteins are reported to range between 15 Å and 30 Å, which is within acceptable limits for efficient energy transfer between donor and acceptor molecules (50). It is anticipated, therefore, that the average distance between Tyr groups in insulin, given as 16.57 Å, will permit efficient intertyrosine resonance energy transfer (28). Indeed, fluorescence-polarization measurements of insulin have established the occurrence of intertyrosine energy transfer (51). It is also expected that Phe residues will contribute to the overall quantum yield of Tyr fluorescence. Resonance energy transfer between Tyr and ANS has been reported (52), and we have also observed that on excitation at 276 nm, the emission spectrum of Tyr in insulin overlaps with the excitation spectrum of unbound ThT (Bekard, I. B. and Dunstan, D. E., unpublished work). Taken together, it can be deduced that the initial structural reorganization preceding insulin fibrillation brings aromatic residues into proximity, hence facilitating energy transfer between donor and acceptor molecules within the protein matrix and in solution. A probable consequence of this dynamic association is the observed quenching of Tyr fluorescence.

Insulin contains three native disulfide bonds that have been established as strong quenchers of intrinsic fluorescence (31). These covalent bonds are known to be highly hydrophobic and shielded from the aqueous environment in native insulin (7,53–55). Tyr is partially hydrophobic, and three out of the four Tyr residues in bovine insulin are located in hydrophobic pockets and involved in hydrophobic interactions resulting in various association states of the protein (13). For this reason, interactions between Tyr residues and disulfide bonds can only occur upon exposure of hydrophobic groups to the solvent. The results show that ANS fluorescence enhancement, which indicates the presence of solvent-exposed hydrophobic regions, occurs in sync with Tyr fluorescence quenching (Fig. 1). This is a clear indication that the ANS binding sites are in proximity to most of the Tyr residues (48), and that exposure of these hydrophobic regions makes Tyr accessible to quenchers. It should be noted that disulfide bonds, which are strong quenchers of intrinsic protein fluorescence, also become solvent-accessible upon insulin denaturation, and their interaction with excited Tyr residues is greatly enhanced.

The results show that Tyr fluorescence quenching persists in the absence of dyes (Fig. 3 *a* and Fig. S1 *a*). This suggests that its occurrence is predominantly a result of intra-/intermolecular singlet-singlet energy transfer between adjacent Tyr residues (51) and, most probably, effective contacts between excited singlet Tyr residues and cystinyl side chains (31). The frequency of these interactions is determined by the heat- and agitation-induced fluidity of the protein matrix resulting from the disruption of hydrophobic pockets and other stabilizing forces that maintain the native protein (56). This is buttressed by the temperature dependence of tyrosine fluorescence, giving ample evidence that the contact quenching mechanism is collisional and not static. The mechanism of Tyr fluorescence quenching by cystine is debated. The suggested possibilities include deactivation of the excited-state molecules via internal conversion or enhanced intersystem crossing to the triplet state (57).

In summary, the start of Tyr fluorescence quenching signifies the emergence of solvent-exposed hydrophobic groups, hence partially folded intermediates, in solution.

## Insulin fibrillation detected via Tyr fluorescence

In 0.1% HCl (pH 1.9), insulin is predominantly dimeric. At 60°C, however, the equilibrium favors the monomeric state and protein denaturation is known to free phenolic groups bound in the native protein. From Figs. 1 and 3 *a* (*inset*), the initial 2 h preceding Tyr fluorescence quenching is the time taken for the dissociation of existing dimers into monomers and disruption of the stabilizing forces of native insulin monomers. The result is thermal and agitation-induced denaturation of monomeric insulin and consequent exposure of hydrophobic regions to the aqueous environment. The start of Tyr fluorescence quenching at ~2 h indicates the emergence of a new structural species, a partially unfolded intermediate, in solution, a conclusion that is buttressed by the results of ANS experiments. This is consistent with reports that partially folded intermediates precede insulin fibrillation (23). The light-scattering profile (Fig. 1) shows that this new structural species associates rapidly into large (oligomeric) aggregates. The Tyr fluorescence phase plot (Fig. 3 *b*) equally detects these aggregates evolving at ~3 h, reaching a maximum concentration at ~12 h. Mass spectrometry studies on amyloidogenic insulin samples incubated at high temperatures revealed that the dissociation of soluble higher oligomers (e.g., dimers) is followed by the formation of high-molecular-weight aggregates, from which fibrils evolve (33).

The emergence of these oligomeric aggregates is attributable to an interplay of electrostatic and hydrophobic interactions that allow self-association of denatured monomers. For example, the chloride ions present in the solvent mask the net positive charge on native insulin at pH 1.9, allowing the coalescence of monomers, via hydrophobic interactions between partially unfolded intermediates, to form a fibril-competent nucleus. This effect of chloride ions is purported to contribute to the precipitation of insulin into a dense network of fibrils (6). The absence of hydrogen-bonded Tyr residues, coupled with the insulin-solvent charge interactions at pH 1.9, supports the hypothesis that the attractive force driving the association of partially unfolded monomers into oligomers at 60°C is hydrophobic in nature. ThT fluorescence begins to increase partway (~5 h, Fig. 1) through the formation of these intermediates, which implies that the oligomers, so formed, begin to polymerize into fibrillar aggregates, and these aggregates become the dominant structural species at 22 h. The saturation of Tyr fluorescence quenching at ~12 h (Fig. 3 *a*, *inset*) indicates that the majority of Tyr residues, hence hydrophobic regions, become solvent-exposed at that time. ThT fluorescence reaches equilibrium after 18 h, which suggests that most of the fibril-competent nuclei are consumed by mature fibrils at that time. Based on these results, it is clear that the major structural changes during insulin aggregation can be detected via Tyr fluorescence.

The sequence of structural changes accompanying insulin fibrillation, and the probes sensitive to each structural transition, as observed in this study, are summarized in Fig. 5. It is noteworthy that the phase plots obtained from intrinsic Tyr fluorescence are sensitive to these structural changes (Fig. 3 *b*).

## Biophysical differences in insulin fibrils formed in the presence or absence of dyes

The AFM images show that the physical appearance of insulin fibrils differs depending on the dye present. Insulin fibrils formed in the absence of ANS or ThT were finer, whereas fibrils formed in the presence of dyes appeared thicker, indicating a higher degree of association. In the case of ANS, the sulphonate group of the dye is negatively charged at pH 1.9 and in complement with chloride ions may mask the net positive charge on insulin, leading to a more significant precipitation of fibrils. ThT, on the other hand, is known to bind along cavities running parallel to insulin fibrils, hence contributing to the overall fibril structure. Indeed, x-ray diffraction studies have confirmed increased morphological variation in insulin fibrils formed in the presence of ThT compared to those formed in the absence of the dye (47). Such structural discrepancies, in addition to the residual $\alpha$-helical structure known to exist in fibrillated insulin, may account for the differences in CD spectra for fibrils formed in the presence and absence of ThT/ANS. It is also likely that the dyes, aside from influencing the fibril structure, also perturb the electron cloud of insulin amide chromophores responsible for the far-UV CD signal; resulting in the observed differences in intensity and peak position (58). It is noteworthy that the techniques applied here do not allow a firm conclusion to be drawn from these observations. Further analysis using techniques such as x-ray diffraction is necessary for concrete comparison of fibrils formed under the different conditions.

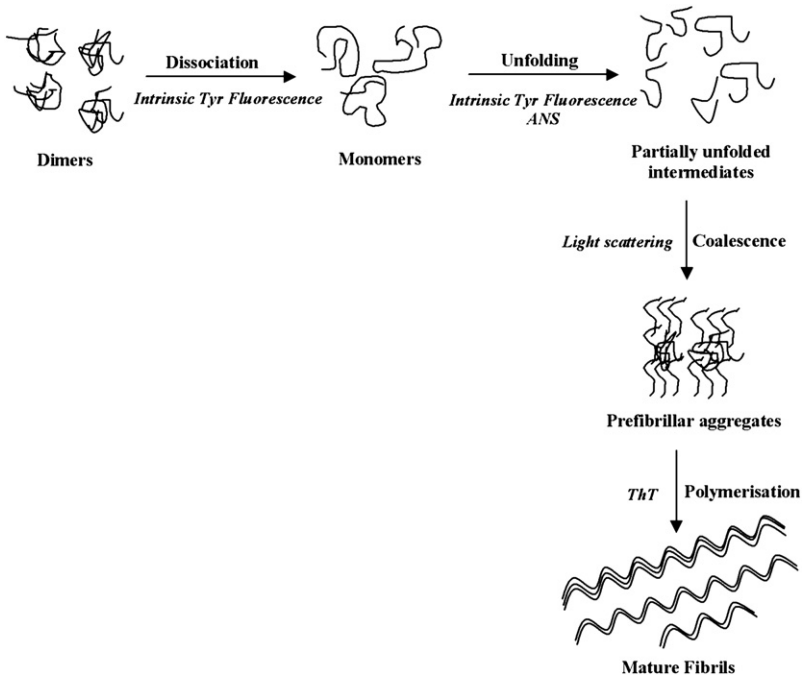


FIGURE 5 Schematic representation of the sequence of on-pathway structural changes accompanying insulin fibrillation.

### Relevance of monitoring insulin aggregation via its intrinsic fluorescence

The nonintrusive but sensitive nature of intrinsic protein fluorescence makes it a versatile tool used in concert with other protein aggregation probes (especially extrinsic probes) to gain additional information on the structural changes associated with insulin deformation and aggregation. The merit in obtaining such critical information from the protein itself cannot be overemphasized. For example, it affords the advantage of directly monitoring changes that occur in the peptide-hormone at the molecular level during aggregation, giving concrete details on the early events preceding fibrillation. This approach is suitable for real-time fluorescence studies conducted in situ. It is noteworthy that the light-scattering technique used in this study only provides qualitative evidence of the association of deformed insulin monomers into larger aggregates. However, its sensitivity to the size increase of insulin aggregates in solution makes it a suitable complementary probe in monitoring protein aggregation.

## CONCLUSION

We have shown that intrinsic Tyr fluorescence can be used to resolve the complex structural modifications associated with insulin fibrillation. The observed Tyr fluorescence quenching during insulin aggregation is attributable to energy transfer between Tyr residues and acceptor molecules (including adjacent Tyr residues, ThT, and ANS) and the likely repetitive collisions between exposed Tyr residues and indole fluorescence quenchers such as the disulfide bonds present in native insulin. There was no evidence of tyrosinate or dityrosine formation during insulin aggregation.

## SUPPORTING MATERIAL

A figure is available at http://www.biophysj.org/biophysj/supplemental/S0006-3495(09)01390-3(XX).

We thank Drs. Kevin Barnham and Deborah Tew for assistance with the CD instrument. We also thank Victoria Hughes for helpful discussions.

Funding for this project was obtained from the Australian Research Council.

## REFERENCES

1. Dobson, C. M. 2003. Protein folding and misfolding. *Nature*. 426: 884–890.
2. Agorogiannis, E. I., G. I. Agorogiannis, A. Papadimitriou, and G. M. Hadjigeorgiou. 2004. Protein misfolding in neurodegenerative diseases. *Neuropathol. Appl. Neurobiol.* 30:215–224.
3. Stefani, M., and C. M. Dobson. 2003. Protein aggregation and aggregate toxicity: new insights into protein folding, misfolding diseases and biological evolution. *J. Mol. Med.* 81:678–699.
4. Brange, J. 1987. Galenics of Insulin: The Physico-Chemical and Pharmaceutical Aspects of Insulin and Insulin Preparations. Springer-Verlag, Berlin/Heidelberg.
5. Brange, J., and L. Langkjaer. 1993. Insulin structure and stability. *In* Stability and Characterization of Protein and Peptide Drugs: Case Histories. Y. J. Wang and R. Pearlman, editors. Springer, New York. 315–350.
6. Whittingham, J. L., D. J. Scott, K. Chance, A. Wilson, J. Finch, et al. 2002. Insulin at pH 2: structural analysis of the conditions promoting insulin fibre formation. *J. Mol. Biol.* 318:479–490.
7. Betz, S. F. 1993. Disulfide bonds and the stability of globular proteins. *Protein Sci.* 2:1551–1558.

8. Lee, C. C., A. Nayak, A. Sethuraman, G. Belfort, and G. J. McRae. 2007. A three-stage kinetic model of amyloid fibrillation. *Biophys. J.* 92:3448–3458.
9. Baker, E. N., T. L. Blundell, J. F. Cutfield, S. M. Cutfield, E. J. Dodson, et al. 1988. The structure of 2Zn pig insulin crystals at 1.5 A resolution. *Philos. Trans. R. Soc. Lond. B Biol. Sci.* 319:369–456.
10. Kline, A. D., and R. M. Justice, Jr. 1990. Complete sequence-specific proton NMR assignments for human insulin. *Biochemistry.* 29:2906–2913.
11. Hua, Q. X., S. E. Shoelson, M. Kochoyan, and M. A. Weiss. 1991. Receptor binding redefined by a structural switch in a mutant human insulin. *Nature.* 354:238–241.
12. Derewenda, U., Z. Derewenda, E. J. Dodson, G. G. Dodson, C. D. Reynolds, et al. 1989. Phenol stabilizes more helix in a new symmetrical zinc insulin hexamer. *Nature.* 338:594–596.
13. Uversky, V. N., L. N. Garriques, I. S. Millett, S. Frokjaer, J. Brange, et al. 2003. Prediction of the association state of insulin using spectral parameters. *J. Pharm. Sci.* 92:847–858.
14. Bryant, C., D. B. Spencer, A. Miller, D. L. Bakaysa, K. S. McCune, et al. 1993. Acid stabilization of insulin. *Biochemistry.* 32:8075–8082.
15. Pillai, O., and R. Panchagnula. 2001. Insulin therapies–past, present and future. *Drug Discov. Today.* 6:1056–1061.
16. Sluzky, V., J. A. Tamada, A. M. Klibanov, and R. Langer. 1991. Kinetics of insulin aggregation in aqueous solutions upon agitation in the presence of hydrophobic surfaces. *Proc. Natl. Acad. Sci. USA.* 88:9377–9381.
17. Nielsen, L., R. Khurana, A. Coats, S. Frokjaer, J. Brange, et al. 2001. Effect of environmental factors on the kinetics of insulin fibril formation: elucidation of the molecular mechanism. *Biochemistry.* 40:6036–6046.
18. Brange, J., L. Andersen, E. D. Laursen, G. Meyn, and E. Rasmussen. 1997. Toward understanding insulin fibrillation. *J. Pharm. Sci.* 86:517–525.
19. Ehrlich, J. C., and I. M. Ratner. 1961. Amyloidosis of the islets of Langerhans: a restudy of islet hyalin in diabetic and nondiabetic individuals. *Am. J. Pathol.* 38:49–59.
20. Dobson, C. M. 2004. Principles of protein folding, misfolding and aggregation. *Semin. Cell Dev. Biol.* 15:3–16.
21. Meredith, S. C. 2005. Protein denaturation and aggregation: cellular responses to denatured and aggregated proteins. *Ann. N.Y. Acad. Sci.* 1066:181–221.
22. Mauro, M., E. F. Craparo, A. Podestà, D. Bulone, R. Carrotta, et al. 2007. Kinetics of different processes in human insulin amyloid formation. *J. Mol. Biol.* 366:258–274.
23. Ahmad, A., V. N. Uversky, D. Hong, and A. L. Fink. 2005. Early events in the fibrillation of monomeric insulin. *J. Biol. Chem.* 280:42669–42675.
24. Levine, 3rd, H. 1999. Quantification of $\beta$-sheet amyloid fibril structures with thioflavin T. *Methods Enzymol.* 309:274–284.
25. Groenning, M., L. Olsen, M. van de Weert, J. M. Flink, S. Frokjaer, et al. 2007. Study on the binding of Thioflavin T to $\beta$-sheet-rich and non-$\beta$-sheet cavities. *J. Struct. Biol.* 158:358–369.
26. Permyakov, E. A., V. V. Yarmolenko, E. A. Burstein, and C. Gerday. 1982. Intrinsic fluorescence spectra of a tryptophan-containing parvalbumin as a function of thermal, pH and urea denaturation. *Biophys. Chem.* 15:19–26.
27. Arutyunyan, A. G., K. M. L'Vov, A. O. Mnatsakanyan, V. A. Oganesyan, and N. V. Shakhnazaryan. 1985. Light quenching of fluorescence of aromatic amino acids. *J. Appl. Spectrosc.* 43:992–994.
28. Teale, F. W. J. 1960. The ultraviolet fluorescence of proteins in neutral solution. *Biochem. J.* 76:38l–388.
29. Bushueva, T. L., E. P. Busel, and E. A. Burstein. 1978. Relationship of thermal quenching of protein fluorescence to intramolecular structural mobility. *Biochim. Biophys. Acta.* 534:141–152.
30. Ahmad, A., I. S. Millett, S. Doniach, V. N. Uversky, and A. L. Fink. 2003. Partially folded intermediates in insulin fibrillation. *Biochemistry.* 42:11404–11416.
31. Permyakov, E. A., editor. 1992. Luminiscent Spectroscopy of Proteins. CRC Press, London.
32. Strickland, E. H., and D. Mercola. 1976. Near-ultraviolet tyrosyl circular dichroism of pig insulin monomers, dimers, and hexamers. Dipole-dipole coupling calculations in the monopole approximation. *Biochemistry.* 15:3875–3884.
33. Nettleton, E. J., P. Tito, M. Sunde, M. Bouchard, C. M. Dobson, et al. 2000. Characterization of the oligomeric states of insulin in self-assembly and amyloid fibril formation by mass spectrometry. *Biophys. J.* 79:1053–1065.
34. Manno, M., E. F. Craparo, V. Martorana, D. Bulone, and P. L. San Biagio. 2006. Kinetics of insulin aggregation: disentanglement of amyloid fibrillation from large-size cluster formation. *Biophys. J.* 90:4585–4591.
35. Burstein, E. A., editor. 1977. Intrinsic Protein Luminescence (Origins and Applications). VINITI, Moscow.
36. Podesta, A., G. Tiana, P. Milani, and M. Manno. 2006. Early events in insulin fibrillization studied by time-lapse atomic force microscopy. *Biophys. J.* 90:589–597.
37. Rayner, D. M., D. T. Krajcarski, and A. G. Szabo. 1978. Excited state acid–base equilibrium of tyrosine. *Can. J. Chem.* 56:1238–1245.
38. Waugh, D. F. 1946. A fibrous modification of insulin. I. The heat precipitate of insulin. *J. Am. Chem. Soc.* 68:247–250.
39. Dusa, A., J. Kaylor, S. Edridge, N. Bodner, D. P. Hong, et al. 2006. Characterization of oligomers during synuclein aggregation using intrinsic tryptophan fluorescence. *Biochemistry.* 45:2752–2760.
40. Whitmore, L., and B. A. Wallace. 2007. Protein secondary structure analyses from circular dichroism spectroscopy: Methods and reference databases. *Biopolymers.* 89:392–400.
41. Brems, D. N., P. L. Brown, L. A. Heckenlaible, and B. H. Frank. 1990. Equilibrium denaturation of insulin and proinsulin. *Biochemistry.* 29:9289–9293.
42. O'Neil, J. D., K. J. Dorrington, D. I. Kells, and T. Hofmann. 1982. Fluorescence and circular-dichroism properties of pig intestinal calcium-binding protein ($M_r = 9000$), a protein with a single tyrosine residue. *Biochem. J.* 207:389–396.
43. Huus, K., S. Havelund, H. B. Olsen, M. van de Weert, and S. Frokjaer. 2005. Thermal dissociation and unfolding of insulin. *Biochemistry.* 44:11171–11177.
44. Dzwolak, W., R. Ravindra, J. Lendermann, and R. Winter. 2003. Aggregation of bovine insulin probed by DSC/PPC calorimetry and FTIR spectroscopy. *Biochemistry.* 42:11347–11355.
45. Kelly, S. M., and N. C. Price. 1997. The application of circular dichroism to studies of protein folding and unfolding. *Biochim. Biophys Acta.* 1338:161–185.
46. Sreerama, N., M. C. Manning, M. E. Powers, J. X. Zhang, D. P. Goldenberg, et al. 1999. Tyrosine, phenylalanine, and disulfide contributions to the circular dichroism of proteins: circular dichroism spectra of wild-type and mutant bovine pancreatic trypsin inhibitor. *Biochemistry.* 38:10814–10822.
47. Groenning, M., M. Norrman, J. M. Flink, M. van de Weert, J. T. Bukrinsky, et al. 2007. Binding mode of Thioflavin T in insulin amyloid fibrils. *J. Struct. Biol.* 159:483–497.
48. Murali, J., and R. Jayakumar. 2005. Spectroscopic studies on native and protofibrillar insulin. *J. Struct. Biol.* 150:180–189.
49. Cowgill, R. W. 1976. Tyrosyl fluorescence in proteins and model peptides. *In* Biochemical Fluorescence: Concepts 2. R. F. Chen and H. Edelhoch, editors. Marcel Dekker, New York. 441–486.
50. Karreman, G., R. H. Steele, and A. Szent-Gyorgyi. 1958. On resonance transfer of excitation energy between aromatic amino acids in proteins. *Proc. Natl. Acad. Sci. USA.* 44:140–143.
51. Weber, G. 1960. Fluorescence-polarization spectrum and electronic-energy transfer in tyrosine, tryptophan and related compounds. *Biochem. J.* 75:335–345.
52. Steiner, R. F. 1984. Location of a binding site for 1-anilinonaphthalene-8-sulfonate on calmodulin. *Arch. Biochem. Biophys.* 228:105–112.

53. Saunders, A. J., G. B. Young, and G. J. Pielak. 1993. Polarity of disulfide bonds. *Protein Sci.* 2:1183–1184.

54. Radzicka, A., and R. Wolfenden. 1988. Comparing the polarities of the amino acids: side-chain distribution coefficients between the vapor phase, cyclohexane, 1-octanol, and neutral aqueous solution. *Biochemistry*. 27:1664–1670.

55. Qiao, Z. S., Z. Y. Guo, and Y. M. Feng. 2001. Putative disulfide-forming pathway of porcine insulin precursor during its refolding in vitro. *Biochemistry*. 40:2662–2668.

56. Eftink, M. R., and C. A. Ghiron. 1975. Dynamics of a protein matrix revealed by fluorescence quenching. *Proc. Natl. Acad. Sci. USA*. 72:3290–3294.

57. Longworth, J. W. 1971. Luminescence of polypeptides and proteins. *In* Excited States of Proteins and Nucleic Acids. R. F. Steiner and I. Weinryb, editors. Plenum Press, New York. 319–483.

58. Havel, A. H., editor. 1996. Spectroscopic Methods for Determining Protein Structure in Solution. VCH Publishers, New York.